NASA/TM—2007-214817

Apparent Relations Between Solar Activity and Solar Tides Caused by the Planets

Ching-Cheh Hung
Glenn Research Center, Cleveland, Ohio

July 2007

NASA STI Program . . . in Profile

Since its founding, NASA has been dedicated to the advancement of aeronautics and space science. The NASA Scientific and Technical Information (STI) program plays a key part in helping NASA maintain this important role.

The NASA STI Program operates under the auspices of the Agency Chief Information Officer. It collects, organizes, provides for archiving, and disseminates NASA's STI. The NASA STI program provides access to the NASA Aeronautics and Space Database and its public interface, the NASA Technical Reports Server, thus providing one of the largest collections of aeronautical and space science STI in the world. Results are published in both non-NASA channels and by NASA in the NASA STI Report Series, which includes the following report types:

- TECHNICAL PUBLICATION. Reports of completed research or a major significant phase of research that present the results of NASA programs and include extensive data or theoretical analysis. Includes compilations of significant scientific and technical data and information deemed to be of continuing reference value. NASA counterpart of peer-reviewed formal professional papers but has less stringent limitations on manuscript length and extent of graphic presentations.

- TECHNICAL MEMORANDUM. Scientific and technical findings that are preliminary or of specialized interest, e.g., quick release reports, working papers, and bibliographies that contain minimal annotation. Does not contain extensive analysis.

- CONTRACTOR REPORT. Scientific and technical findings by NASA-sponsored contractors and grantees.

- CONFERENCE PUBLICATION. Collected papers from scientific and technical conferences, symposia, seminars, or other meetings sponsored or cosponsored by NASA.

- SPECIAL PUBLICATION. Scientific, technical, or historical information from NASA programs, projects, and missions, often concerned with subjects having substantial public interest.

- TECHNICAL TRANSLATION. English-language translations of foreign scientific and technical material pertinent to NASA's mission.

Specialized services also include creating custom thesauri, building customized databases, organizing and publishing research results.

For more information about the NASA STI program, see the following:

- Access the NASA STI program home page at *http://www.sti.nasa.gov*

- E-mail your question via the Internet to *help@sti.nasa.gov*

- Fax your question to the NASA STI Help Desk at 301–621–0134

- Telephone the NASA STI Help Desk at 301–621–0390

- Write to:
  NASA Center for AeroSpace Information (CASI)
  7115 Standard Drive
  Hanover, MD 21076–1320

NASA/TM—2007-214817

Apparent Relations Between Solar Activity and Solar Tides Caused by the Planets

Ching-Cheh Hung
Glenn Research Center, Cleveland, Ohio

National Aeronautics and
Space Administration

Glenn Research Center
Cleveland, Ohio 44135

July 2007

This report is a formal draft or working paper, intended to solicit comments and ideas from a technical peer group.

This report contains preliminary findings, subject to revision as analysis proceeds.

Level of Review: This material has been technically reviewed by technical management.

Available from

NASA Center for Aerospace Information
7115 Standard Drive
Hanover, MD 21076–1320

National Technical Information Service
5285 Port Royal Road
Springfield, VA 22161

Available electronically at http://gltrs.grc.nasa.gov

Apparent Relations Between Solar Activity and Solar Tides Caused by the Planets

Ching-Cheh Hung
National Aeronautics and Space Administration
Glenn Research Center
Cleveland, Ohio 44135

Summary

A solar storm is a storm of ions and electrons from the Sun. Large solar storms are usually preceded by solar flares, phenomena that can be characterized quantitatively from Earth. Twenty-five of the thirty-eight largest known solar flares were observed to start when one or more tide-producing planets (Mercury, Venus, Earth, and Jupiter) were either nearly above the event positions (<10° longitude) or at the opposing side of the Sun. The probability for this to happen at random is 0.039 percent. This supports the hypothesis that the force or momentum balance (between the solar atmospheric pressure, the gravity field, and magnetic field) on plasma in the looping magnetic field lines in solar corona could be disturbed by tides, resulting in magnetic field reconnection, solar flares, and solar storms. Separately, from the daily position data of Venus, Earth, and Jupiter, an 11-year planet alignment cycle is observed to approximately match the sunspot cycle. This observation supports the hypothesis that the resonance and beat between the solar tide cycle and nontidal solar activity cycle influences the sunspot cycle and its varying magnitudes. The above relations between the unpredictable solar flares and the predictable solar tidal effects could be used and further developed to forecast the dangerous space weather and therefore reduce its destructive power against the humans in space and satellites controlling mobile phones and global positioning satellite (GPS) systems.

Introduction

Observing the Sun has been an important task since the beginning of human history. Observation is becoming increasingly important as human activity advances into space, going beyond the Earth's magnetic field and atmosphere, and humans are directly exposed to the dangerous space weather caused by solar activity. In the past, large solar storms have disrupted communications and damaged ground-level electrical equipment. Recently, it caused misreading of meters, degradation of solar panels and loss of satellites, including the loss of the $200 million Telstar 401 in 1997 (ref. 1). It will almost certainly be more troubling in the future, when the communication satellites controlling items used by the general public (e.g., mobile phones, the Internet, and GPS systems) could be disabled by a solar storm for days. Additionally, the solar storms (the "rains of ions and electrons") will certainly be a factor affecting the activity of human exploration on the Moon.

The current defense against such natural solar events is illustrated by the event of October 2003: After large sunspot groups were observed, solar storm warnings were issued and satellite operations were shut down in time to limit the damage (ref. 2). This strategy is not ideal because a large solar storm cannot be foreseen until the large sunspot groups appear. Long-term forecasting is therefore limited. In addition, some solar storms have not come from regions of giant sunspot groups. They came without warning and are even more damaging because everyone is caught unprepared. An example of damage caused by such surprising storms was the loss of the above-mentioned communication satellite Telstar 401 in 1997 (ref. 1).

Better understanding of solar activity is desirable in order to better forecast space weather to protect human activities on Earth as well as human lives in space. Current thinking is that much of the solar activity is a direct result of the variation in the magnetic fields in the solar atmosphere. In the Sun's photosphere (visible surface), the magnetic fields are highly concentrated bundles that are widely

distributed, but they cover only a few percent of the photosphere's surface. Hot electrified gas (plasma) is trapped within the closed loops of intense magnetic fields to form the bundles. These intense magnetic field regions are numerous and small during solar inactive periods, but coalesce to form large sunspots during the solar active periods (ref. 3). The magnetic fields are generated at the tachocline, the sharp layer between the differentially rotating convection zone and the uniform-rotating radiative zone. The tachocline is below the photosphere by about 30 percent of the Sun's radius (ref. 3). The magnetic fields may extend out from the photosphere into the corona, the region above the photosphere where some plasma accelerates into space. Reconnection of the magnetic fields in the corona was observed during solar flares, which resulted in solar storms experienced on Earth (ref. 2).

One source of the magnetic field variations in the vast solar atmosphere from tachocline to corona is believed to be the result of solar differential rotation (ref. 3). Another possible source of the variation in the solar magnetic field (the sunspots) that had been studied in the past century, but is currently considered unlikely, is the solar tides caused by the planets (refs. 4 to 6). Today's textbooks mention neither the possible relations between the tide and solar activity nor the research in this area that has been done in the past century. Unfortunately, the belief that such relations do not exist has prevented scientists from taking advantage of a larger and more accurate satellite data of the Sun collected since 1970s. A statistical analysis of such data—solar flare data obtained from GOES satellites during the last three solar cycles and pre-1975 ground observations that are believed to be accurate—is presented in detail in this report. A clear relationship between solar flares and the solar tides caused by the planets is seen. Also in this report previous research in this area is summarized and discussed, and the relation between the planet alignment cycle and sunspot cycle that has previously been examined and disregarded is further investigated.

Previous Work on Tide-Solar Activity Relations: Summary and Discussions

Cycles of Venus, Earth, and Jupiter alignment were found to have an 11- or 22-year period (refs. 4 and 5). This suggests the possibility of a resonance between the sunspot cycle and the planet alignment cycle. Increased radio and x-ray emissions were observed when the planets were aligned during the 2-month period leading to the large sunspot groups or major solar flares (ref. 6). This suggests a possible thermal effect in the development of tides on the solar surface. Correlation between the position of sunspots at their first appearance and the heliocentric longitude of Mercury, Venus, and Jupiter has been noted (ref. 7).

If it is true, then the unpredictable solar activity could be related to the predictable planet positions, and the capacity of solar activity and space weather forecasts would be increased. This includes the solar activities at the far side from Earth. However, such relation could not be confirmed in many other reports. For example, for the group of more than 1000 solar flares during 1955 and 1961, the correlation between the solar flare and the heliocentric longitude of Venus and Jupiter could not be found (ref. 8). Today, the relation is widely considered unlikely because the tides are believed to be too small (tide-driving gravity caused by the Earth on the Sun/Sun's own gravity = 10^{-12}) (ref. 9), too regular, and unrelated to the solar activity in terms of cycle period (10.4 years due to planet alignment or 11.87 years due to tide potential versus 11.0 years for observed solar activity) (ref. 10), and too regular to explain the Maunder minimum—the 70-year-period of 1645 to 1715 AD when the planets moved regularly, but few sunspots were observed (ref. 9).

Some of the above research (refs. 9 and 10) may have over-emphasized the tide-Jupiter relation, which resulted from the use of maximum tide potential as the criterion of tidal effect and resulted in questionable conclusions. The energy to cause the tidal effect would more likely be proportional to the variation of the tide potential on the active regions as the Sun rotates, not by the magnitude of the tide potential itself. This variation will cause transfer between potential energy and other forms of tide energy. At the events when Jupiter was closest to the Sun, both maximum and minimum tide potentials experienced by the active region over one solar rotation were high. The tidal effects at these events would

be considered high in those reports, but in fact may be insignificant because the variation (i.e., maximum minus minimum) of tide potential in one solar rotation could be small.

In addition, the possibility of resonance and beat occurring between the solar tide cycle caused by planet alignment and the cycle of nontidal solar activity was not discussed in the above research reports. The irregular cycle of nontidal solar activity could be magnified by resonating with the cycle of regular solar tide caused by the planet alignment when the two cycles are in step, and be reduced to a state of Maunder Minimum when they are out of step.

Furthermore, the general belief that "the solar tide is insignificant because the tide-driving gravities are too small to affect the solar activities" should be questioned considering (1) the tide on the Sun's atmosphere could be comparable to that on the Earth's atmosphere by the Sun and Moon, which has a tide-driving gravity of about 10^{-7} of the Earth's gravity and (2) the tidal influence at solar corona could be much more significant than the tidal influence at the visible solar surface. These are explained as follows:

(1) Since the tidal phenomena on Earth are known to exist and are understood, they were used as reference points with which to compare the possible tidal phenomena on the Sun (see appendix A). The solar atmosphere's smaller tide gravity to regular gravity ratio relative to the Earth atmosphere's ($10^{-12}/10^{-7} = 10^{-5}$) could be balanced by its larger size (10^2 by radius for larger horizontal tide and $>10^3$ by depth for larger vertical tide). The longer rotation period of the Sun as viewed by the planets (25 to 35 days) relative to the rotation period of the Earth (1 day) also suggests the Sun's tide could be bigger: tide-driving gravity from these planets is experienced by the Sun for a longer time in comparison. An analysis of how orbiting period affects the atmospheric tides is briefly described in appendix B.

(2) It is noted that in solar corona the visible looping magnetic field can be above the visible solar surface by 2 to 3 times the solar radius, and visible streamers can be seen above the visible solar surface at more than 10 times the solar radius. At that height the tidal influence on the plasma would be much more significant than the tidal influence at visible solar surface (i.e., the ratio of the tide-driving gravity to the Sun's own gravity $>> 10^{-12}$) because plasma would experience higher tide-driving gravity (proportional to the distance from the Sun's center, see appendix A) and lower gravity due to Sun's own mass (inversely proportional to the square of the distance from the Sun's center).

Current Work

Solar activities are believed to be the results of many different forces, and the strongest solar activities take place when all forces act together. Therefore, if the tide-driving gravities by the planets could be influential, they would have to be in action at the time of the strongest solar activities.

In the research presented in this report, it is hypothesized that the tide-driving gravities by the planets could be one of the forces that cause the solar activity observed from Earth. This means the tide-driving gravities could be sufficiently large to cause the molecules, electrons, and ions to mix or shift positions in at least part of the vast region between the corona and the tachocline, especially when the solar tides caused by the individual planets converge and diverge as the planets come into and out of alignment. Therefore, the pressure differences between the plasma in the magnetic fields and the materials outside would change because of their different environmental states. Corresponding to a variation in state, the magnetic field could move, change shape, merge, or disperse, and the solar activity could increase or decrease. Specifically in the looping magnetic field lines in solar corona, the force or momentum balance between the solar atmospheric pressure, the gravitational field, and the magnetic field on masses of plasma in the magnetic field could be disturbed by tides, resulting in magnetic field reconnection and solar flares (ref. 2).

The current research uses data and knowledge acquired since the above reports were published in the 1970s to reexamine the possible relations between solar tides caused by the planets and the observed solar activities. It includes two parts. The first part is similar to Schuster's (ref. 7) and Dingle, Van Hoven, and Sturrock's (ref. 8), where a correlation between the position of various solar events and the heliocentric longitude of Mercury, Venus, and Jupiter were each examined, respectively. Here, correlation between

the position of the solar flares and the heliocentric longitude of Mercury, Venus, Earth, and Jupiter as one group was examined. The second part of this report is similar to Wood's report in 1972 (ref. 5), which concluded the cycle of the alignment of Venus, Earth, and Jupiter was very similar to the sunspot cycle during 1800 to 1970. That report was later described as an "incomplete tidal theory" because of numerous defects (refs. 9 and 10). In this report Wood's idea is revisited and further developed for the period from 1840 to 2005 using a new method and a new interpretation to prevent the noted defects.

The tide-driving gravity equations that are relevant to this research are summarized and briefly discussed in appendix A. Four of the planets (Mercury, Venus, Earth, and Jupiter) are known to be the major tide-producing planets (refs. 4, 5, 7, 9, and 10) for the Sun. The tide-driving gravities of Venus and Jupiter are about equal and are about twice those of Earth and Mercury (app. A). The planets discussed in the remainder of this report will be these four planets, as the tide-driving gravities of all other planets are negligible.

The potential of using the planet position-solar activity relations to forecast space weather is briefly acknowledged at the end of this report.

Apparent Relations Between Planet Positions and Solar Flares

Before the space age, numerous solar flares were observed. However, the accuracy of solar flare magnitude and event positions during that time is questionable except for those flares that were intensively studied—that is, those associated with solar super storms. The solar flare events investigated in this research include 20 flares that caused nine time periods of historically large solar storms. These include seven time periods described in the review report by Shea and Smart in reference 11 (February 28, 1942; July 25, 1946; November 19, 1949, February 10, 17, and 23, 1956; July 10, 14 and 16, 1959; November 10, 12, and 15, 1960; and August 2, 4, and 7, 1972); the historical large flares of September 1, 1859 (ref. 12); and the recent October 28 and 29, November 2 and 4, 2003, event (ref. 13). In addition, the 30 largest solar flares (ref. 14) in the last three solar cycles and recorded by GOES (Geostationary Operational Environmental Satellite) (ref. 13) were also studied and summarized briefly.

The planets' heliocentric ecliptic positions[1] (ref. 15) at the moment of the largest solar flares (where event positions and event time were known) were collected. The source flare's heliocentric ecliptic positions were calculated from the heliocentric ecliptic position of the Earth and the heliographic positions of the events as viewed from the Earth (refs. 13 and 16 to 18) according to the methods of coordinate transformation described by Hapgood (ref. 19) and Thompson (ref. 20) and summarized in appendix C.

Largest Historical Solar Flares

Table I summarizes the positions of the 20 large historical solar flare events and of the planets at the flare onset time. In 17 of the 20 events, the event flared explosively near the locations where the planets were either directly (<10° longitude) overhead or on the opposite side—aligned through the center—of the Sun (underfoot). These are the likely locations of disturbance of the force or momentum balance on plasma trapped in the looping magnetic field lines extended into corona because the tidal effects caused by the individual planets reached peak and reverse courses there.

Ironically, the largest flare in this category (November 4, 2003, X28) was the one of the three that flared at a position where there was no planet near the overhead or underfoot of the event position. This flare appears to have its own type of flare mechanism, as the active region flared explosively three times within the previous 8 days, when it was at the high tide of Earth, Mercury, and Venus, respectively, before it had the largest final explosion. It is noted that the most influential planets—Venus and Jupiter—were about 30° from either side of the event position at the time of the solar flare.

[1]The angle of the planet's position in polar coordinates where the Sun is at the origin and the Earth's orbit is the plane of reference. The Earth's position at the 2000 AD equinox is 180°.

TABLE I.—PLANET POSITIONS DURING FLARES OF THE NINE LARGEST SOLAR FLARE EVENTS

Event period number	Event position[a]		Flare intensity[b]	Event onset time[c]		Heliocentric ecliptic longitude,[d,e] deg					Event position relative to nearest high-tide position	
				Date	UT	M	V	E	J	F	Deviation,[f] deg	Planet[e]
1	20N	15E	-------	1859 Sept. 01	11:20	352.4	143.3	340.4	101.2	326.1	3	V
2	7N	4E	3	1942 Feb. 28	12:42	215.4	176.0	160.1	84.3	155.8	–4	E
3	20N	15E	3+	1946 July 25	15:04	285.4	232.6	302.8	211.1	289.6	4	M
4	2S	70W	3+	1949 Nov. 19	10:30	233.0	14.2	57.5	308.5	127.5	–1	J
5	22N	90E	3?	1956 Feb. 10	21:10	192.4	58.1	141.7	146.7	49.1	–9	V
	20N	4W	3	1956 Feb. 17	11:00	214.5	68.7	148.4	147.2	151.5	3, 4	E, J
	23N	80W	[g]3	1956 Feb. 23	3:31	231.6	77.9	154.1	147.7	237.1	5	M
6	20N	60E	3+	1959 July 10	2:06	235.5	254.5	287.7	241.8	230.0	–5	M
	17N	4E	[g]3+	1959 July 14	3:25	246.8	260.9	291.5	242.1	288.9	–3	E
	16N	31W	3+	1959 July 16	21:14	254.4	265.3	294.2	242.3	325.5	31	E
7	28N	28E	3	1960 Nov. 10	10:09	62.6	317.7	48.6	281.1	18.9	–30	E
	27N	4W	[g]3+	1960 Nov. 12	13:15	75.9	321.0	50.7	281.2	51.7	1	E
	25N	35W	3	1960 Nov. 15	2:07	91.9	325.1	53.3	281.4	85.0	–7	M
8	13N	27E	2B	1972 Aug. 02	19:58	299.2	340.0	311.0	277.0	285.0	8	J
	14N	8E	3B	1972 Aug. 04	6:20	303.8	342.3	312.3	277.1	305.1	1, –7	M, E
	14N	36W	[g]3B	1972 Aug. 07	14:43	315.0	347.6	315.6	277.4	351.2	4	V
9	16S	8E	X17.2	2003 Oct. 28	8:32	220.7	258.9	34.5	154.1	28.3	–6	E
	15S	2W	X10.0	2003 Oct. 29	20:25	225.2	261.3	36.0	154.2	40.0	4, –5	E, M
	14S	56W	X8.3	2003 Nov. 02	16:41	236.3	267.4	39.8	154.5	97.5	10	V
	19S	83W	[g]X28.0	2003 Nov. 04	19:08	242.2	270.7	41.9	154.6	126.5	–28	J

[a]N, S, E, and W are north, south, east, and west, respectively.

[b] Intensities for event periods 1 through 8 are characterized by optical light emissions. Number indicates size of flare and letter indicates brightness (B is brilliant). For event period 9, intensity is characterized by x-ray emissions. The x-ray intensity is categorized using letters (by order of X, M, C, B, and A, strongest to weakest) and further ranked by numbers.

[c]UT is universal time.

[d]Location of Earth at vernal equinox of 2000 AD is 180°.

[e]M, V, E, J, and F are Mercury, Venus, Earth, Jupiter, and flare, respectively.

[f]Positive deviation means event position was ahead (to the west) of high-tide position. Negative deviation means event position was behind (to the east) of high-tide position. High-tide position is defined as position where the associated planet is either overhead or underfoot.

[g]Largest solar flare in its event period.

The other two of the three solar flares that exploded at a position where there was no planet near the overhead or underfoot of the event position seem to have this type of flare mechanism, too. That is, they also had the active regions flared explosively once or more within the previous 7 days, when it was at the high tide of one planet, before it had the large explosion about 30° from a planet.

Table II summarizes the planet positions and solar flare event positions for the 10 largest flares in the last three solar cycles. Again, the majority of the events had an onset time when there were planets nearly directly overhead or underfoot. Combining this table with the eight large pre-1975 solar flares (one largest solar flare from every one of the eight event periods of solar storms described in table I), among the 18 events described there, 15 happened within 10° from the overhead or underfoot points of at least one of the four planets considered in this research. The probability for a solar flare to start at such location by chance is $1–[1–(10°\times4)/360°]^4$, or 37.57 percent. For this to happen 15 or more out of 18 times at random, the probability is calculated to be about 0.0093 percent according to the binomial probability law. That is,

$$\sum_{n=15}^{18}\left[\frac{18!}{n!(18-n)!}\right](0.3757)^n(1-0.3757)^{18-n}=0.000093=0.0093\% \qquad (1)$$

TABLE II.—PLANET POSITIONS AND SOLAR FLARE EVENT POSITIONS AT TIME OF 10 LARGEST SOLAR FLARES IN LAST THREE SOLAR CYCLES

Event position[a]		Flare intensity[b]	Event onset time[c]		Heliocentric ecliptic longitude,[d,e] deg					Event position relative to nearest high-tide position	
			Date	UT	M	V	E	J	F	Deviation,[f] deg	Planet[e]
19S	83W	X28.0	2003 Nov. 04	19:08	242.2	270.7	41.9	154.6	126.5	–28	J
17N	68W	X20.0	2001 Apr. 02	21:13	304.7	195.5	193.2	77.2	263.5	6	J
18S	84W	X20.0	1989 Aug. 16	0:59	232.1	230.0	323.3	84.5	49.3	–1, –3	V, M
16S	8E	X17.2	2003 Oct. 28	8:32	220.7	258.9	34.5	154.1	28.3	–6	E
11S	77E	X17.0	2005 Sept. 07	16:54	124.1	268.8	345.1	205.8	266.6	–2	V
35N	69E	X15.0	1989 Mar. 06	13:38	269.4	328.6	166.1	70.4	91.9	3	M
20N	46E	X15.0	1978 July 11	10:50	210.9	215.6	289.1	108.2	245.2	30	V
20S	85W	X14.4	2001 Apr. 15	12:48	353.0	215.9	205.6	78.3	288.4	30	J
12S	43E	X13.0	1984 Apr. 24	23:51	221.1	2.0	215.2	272.9	172.0	–10	V
27S	10E	X13.0	1989 Oct. 19	12:03	144.6	332.2	26.2	90.1	18.5	–8	E

[a]N, S, E, and W are north, south, east, and west, respectively.
[b]Higher numbers indicate higher intensity of x-ray emissions.
[c]UT is universal time.
[d]Location of Earth at vernal equinox of 2000 AD is 180°.
[e]M, V, E, J, and F are Mercury, Venus, Earth, Jupiter, and flare, respectively.
[f]Positive deviation means event position was ahead (to the west) of high-tide position. Negative deviation means event position was behind (to the east) of high-tide position. High-tide position is defined as the position where the associated planet is either overhead or underfoot.

This number means the relation between the solar flare position and the planet or vertical tide position is real, with a confidence level of nearly 4 standard deviations.

The three flare events (July 11, 1978; April 15, 2001; and November 4, 2003, in table II) together with the two pre-1975 events (July 16, 1959, and November 10, 1960, in table I) that did not happen near the planets' overhead or underfoot positions were examined. Interesting similarities among their planet position-event position relations can be found: In all five events, the sunspot groups had flared explosively several times 3 to 7 days before (refs. 13 and 14), when they were at the high tides of one or two aligned or nearly aligned planets (ref. 15, table III). In all five events, at the time of the final major flares, the event positions were about 30° away from the nearest planets. Whether these similarities were the results of coincidence remains to be determined.

To put the observations together, it appears that the large sunspots, which had already been very explosive, were sent to the location directly under the individual planets (some of them aligned) or their opposing ends by the rotation of the Sun. These are the locations where the tides caused by the individual planets peak out and reverse courses. The sunspot exploded there, sometimes only partly, became even more unstable, and eventually had the largest flare about 30° from the closest planet as it entered into the area where both vertical and horizontal tide-driving gravity are significant (app. A).

Table IV summarizes the 11th to 30th largest flares during the same period (X9 to X13). In this group, 10 out of 20 events flared within 10° from the overhead or underfoot points of at least one of the four tide-producing planets. This is more frequent than the 37.57-percent probability calculated above, but less frequent than the 15 out of 18 for the largest flares. It appears that the contribution of solar tides in the process of solar flaring was essential to generate the largest solar flares, but was not as necessary for the generation of smaller solar flares.

Unlike the top 10 solar flares described in table II, table IV shows that among the top 11th to 30th solar flares where no planets were within 10° from the flare positions, the similarities in their planet positions relative to the event positions are not obvious. This again indicated that the contribution of solar tides in the process of solar flaring was less necessary for the generation of smaller solar flares.

TABLE III.—PLANET AND SOLAR FLARE POSITIONS FOR MAJOR FLARE EVENTS WHERE THE LARGEST FINAL FLARE WAS APPROXIMATELY 30° FROM NEAREST HIGH-TIDE POSITION

Event position[a]		Flare intensity[b]	Event time[c]		Heliocentric ecliptic longitude, deg[d,e]					Event position relative to nearest high-tide position	
Latitude	Longitude		Date	UT	M	V	E	J	F	Deviation,[f] deg	Planet[e]
November 4, 2003, event											
21S	88E	X5.4	2003 Oct. 23	8:03:00	204.8	251.0	29.5	153.7	299.4	–34	J
17S	84E	X1.1	2003 Oct. 23	19:36:00	206.4	251.7	29.9	153.7	304.5	–29	J
15S	44E	X1.2	2003 Oct. 26	5:00:00	214.1	255.5	32.3	153.9	348.7	15	J
16S	8E	X17.2	2003 Oct. 28	8:32:00	220.7	258.9	34.5	154.1	28.3	–6	E
15S	2W	X10.0	2003 Oct. 29	20:25:00	225.2	261.3	36.0	154.2	40.0	4, –5	E, M
14S	56W	X8.3	2003 Nov. 02	16:41:00	236.3	267.4	39.8	154.5	97.5	10	V
19S	83W	X28.0	2003 Nov. 04	19:08:00	242.2	270.7	41.9	154.6	126.5	–28	J
July 11, 1978, event											
17N	79E	M3	1978 July 08	19:36:00	202.3	211.4	286.6	108.0	209.1	–2, 7	V, M
19N	68E	X3	1978 July 08	23:29:00	202.8	211.6	286.7	108.0	220.8	9, 18	V, M
18N	63E	M5	1978 July 10	1:31:00	206.4	213.4	287.8	108.1	226.8	13, 20	V, M
18N	58E	X3	1978 July 10	6:16:00	207.1	213.7	288.0	108.1	232.1	18, 25	V
19N	54E	M7	1978 July 10	16:16:00	208.4	214.4	288.4	108.2	236.6	22	V
20N	46E	X15	1978 July 11	10:50:00	210.9	215.6	289.1	108.2	245.5	30	V
April 15, 2001, event											
21S	83E	X1.2	2001 Apr. 03	2:53:00	305.4	195.9	193.4	77.2	112.6	–13	M
21S	31E	X5.6	2001 Apr. 06	18:59:00	318.0	201.8	197.0	77.5	166.2	28	M
21S	4W	M7.9	2001 Apr. 09	15:06:00	328.4	206.4	199.8	77.8	202.6	3, –4	E, V
23S	9W	X2.3	2001 Apr. 10	4:46:00	330.6	207.3	200.4	77.8	207.7	0, 7	V, E
19S	43W	X2.0	2001 Apr. 12	8:50:00	339.3	210.8	202.5	78.0	243.3	–15	J
20S	85W	X14.4	2001 Apr. 15	12:48:00	353.0	215.9	205.6	78.3	288.4	30	J
July 16, 1959, event											
20N	60E	3+	1959 July 10	2:06	235.5	254.5	287.7	241.8	230.0	–6, –12	M, J
17N	4E	3+	1959 July 14	3:25	246.8	260.9	291.5	242.1	288.9	–3	E
16N	31W	3+	1959 July 16	21:14	254.4	265.3	294.2	242.3	325.5	31	E
November 10, 1960, event											
Active region at far side before Nov. 5, 1960											
21	–83	2+	1960 Nov. 5	20:04:00	35.0	310.4	44.0	280.7	322.1	12	V
28	–28	3	1960 Nov. 10	10:09:00	62.6	317.7	48.6	281.1	18.9	–30	E

[a]N, S, E, and W are north, south, east, and west, respectively.
[b]X-class flares are 10 times more intense than M-class. Higher numbers indicate higher intensity of x-ray emissions.
[c]UT is universal time.
[d]Earth location at vernal equinox of 2000 AD is 180°.
[e]M, V, E, J, and F are Mercury, Venus, Earth, Jupiter, and flare, respectively.
[f]Positive deviation means event position was ahead (to the west) of high-tide position. Negative deviation means event position was behind (to the east) of high-tide position. High-tide position is defined as the position where the associated planet is either overhead or underfoot.

TABLE IV.—PLANET POSITIONS AND SOLAR FLARE EVENT POSITIONS AT TIME OF 11th TO 30th LARGEST SOLAR FLARES IN LAST THREE SOLAR CYCLES

Event position[a]		Flare intensity[b]	Event onset time[c]		Heliocentric ecliptic longitude,[d,e] deg					Event position relative to nearest high-tide position	
			Date	UT	M	V	E	J	F	Deviation,[f] deg	Planet[e]
10S	24E	X12.9	1982 Dec. 15	1:41:00	310.8	286.7	83.0	233.6	60.0	6	J
9S	25E	X12.0	1982 Jun. 06	16:06:00	264.6	339.4	255.9	218.9	229.8	11	J
25N	90E	X12.0	1991 June 01	14:49:00	356.8	198.6	250.7	138.5	160.3	–17	M
30N	70E	X12.0	1991 June 04	3:37:00	9.1	202.7	253.2	138.7	184.5	–5	M
33N	44E	X12.0	1991 June 06	0:36:00	18.8	205.7	255.0	138.9	214.6	9	V
31N	17W	X12.0	1991 June 11	1:49:00	47.6	213.9	259.8	139.3	280.4	21	E
33N	69W	X12.0	1991 June 15	4:35:00	73.0	220.5	263.7	139.6	333.4	14	J
8S	21W	X10.1	1982 Dec. 17	17:40:00	320.1	290.9	85.7	233.8	107.0	–4	V
9S	52E	X10.1	1984 May 20	21:55:00	294.8	43.4	240.3	275.0	187.9	–36	V
15S	2W	X10.0	2003 Oct. 29	20:25:00	225.2	261.3	36.0	154.2	40.0	4, –5	E, M
16S	78E	X10.0	1991 Jan. 25	6:30:00	230.4	353.4	124.9	128.4	48.6	–2	M
34N	4E	X10.0	1991 June 09	1:34:00	35.7	210.6	257.9	139.1	258.6	1	E
17N	73E	X9.8	1982 July 09	7:24:00	25.0	31.4	287.0	221.4	215.5	4, –6	V, J
26S	92W	X9.8	1989 Sept. 29	10:01:00	25.2	300.4	6.4	88.3	101.4	13	J
26S	28E	X9.4	1991 Mar. 22	22:41:00	96.5	84.1	181.9	132.9	154.5	22	J
18S	63W	X9.4	1997 Nov. 06	11:43:00	269.5	2.1	44.1	324.9	109.0	20	M
33N	78W	X9.3	1990 May 24	20:43:00	282.1	320.5	243.5	108.4	323.1	3	V
12S	74E	X9.0	1980 Nov. 06	3:32:00	58.1	134.5	44.2	175.1	329.5	15	V
24S	93W	X9.0	1992 Nov. 02	1:54:00	322.3	310.1	40.0	178.7	134.5	4, –8	V, M
5S	59E	X9.0	2006 Dec. 05	10:35:00	188.9	275.7	73.1	240.5	14.6	5	M

[a]N, S, E, and W are north, south, east, and west, respectively.
[b]Higher numbers indicate higher intensity of x-ray emissions.
[c]UT is universal time.
[d]Location of Earth at vernal equinox of 2000 AD is 180°.
[e]M, V, E, J, and F are Mercury, Venus, Earth, Jupiter, and flare, respectively.
[f]Positive deviation means event position was ahead (to the west) of high-tide position. Negative deviation means event position was behind (to the east) of high-tide position. High-tide position is defined as the position where the associated planet is either overhead or underfoot.

Combining the solar flare events in tables I, II, and IV (X9.0 and larger), the solar flares started at less than 10° from the nearest planets 25 out of 38 times. The probability for this to happen by chance is again calculated. It is still very low, at 0.039 percent. This means the relation is real with a confidence level of about 3 standard deviations.

An alternative way to judge the statistical significance of these events to occur as given above is by examining the probability of all events to happen in one single circumstance. This involves a probability calculation to look at the maximum deviation (table IV) between the event longitude and the nearest planet longitude, 36°. If the solar flare and the tides caused by the planets are not related, the probability for a solar flare to start at 36° or less from the nearest planet is $1–[1–(36°\times4)/360°]^4$, or 87.04 percent. The probability for this to happen 38 times without exception is calculated to be about $(0.8704)^{38}$ = 0.51 percent. This means the relation is real with a confidence level of about 2.6 standard deviations.

The above results give a way to forecast the times of the largest solar flares (X9.0 and larger) when giant sunspots appear: They are most likely to start when these sunspots rotate into a region where at least one of the four tide-producing planets is either overhead or underfoot (within 10° longitude). They are least likely to occur when these sunspots are at 36° longitude or further away from the overhead or underfoot points of all these four planets.

This method may be useful to forecast some large solar flares at far side of the Sun. Such flares may affect space weather near Earth, but are not able to be seen from Earth. This method is an illustration that forecasting of solar flares after the appearance of sunspots is possible upon examining the tide behaviors (see app. D). Longer term forecasting of solar activity may be possible upon examining tide behaviors over the long term and further developing the theory of solar tide. The following section is an example of such examination to study the relation between sunspot cycles and planet alignment.

Planet Alignment Cycles and Solar Cycles

Resonance

The solar activity may be magnified if a resonance between nontidal activity and the solar tides can be established. The greater the resonance, the more dominant the tide effect is. If, during every 11-year solar activity cycle defined by the sunspot activity, there is a continuous time period where the solar tides caused by the planets are large and another phase where the solar tides are small, then a resonance between the cycle of these solar tides and the cycle of nontidal solar activity can be established.

The existence of such resonance is possible because 11-year cycles resulting from the planet movements have been identified before. Wood took the alignment data for Venus, Earth, and Jupiter once in every 0.8 years during 1800 to 2000 AD periods. He concluded the cycle of the alignment of these three planets was very similar to the sunspot cycle up to the time when he published the paper in 1972 (ref. 5). Okal and Anderson considered Wood's conclusion an artifact of the calculation because the effects of partial planet lineup and the role of Mercury were not considered, and the data points were too few. They concluded the period of the maximum tide potential cycle (very regular 11.9 years) shows no sign of beat, was due to the eccentricity of Jupiter's orbit, and was unrelated to the sunspot cycle. They also concluded the planet alignment within 10° was not associated with drastic tidal effects (ref. 10).

However, their use of maximum tide potential as the criterion of large tidal effect may result in questionable conclusions. As described in the Previous Work section of the Introduction to this report, the energy to cause the tidal effect would more likely be proportional to the variation of the tide potential on the active regions as the Sun rotate, not by the magnitude of the tide potential itself. This is because the variation will cause transfer between potential energy and other forms of tide energy.

In the following section of this report, instead of maximum tide potential, analysis of alignment and near-alignment of all planets was conducted. It is thought that such alignment would most likely have significant tidal effect because it ensures a single tide that, although not necessarily having the highest tide peak, is a broad global tide that, in one solar rotation, will have a significant variation in tide potential. In addition, the converging, and then diverging, of all tides caused by the individual planets being examined may provide the pressure differences needed to change the movement of plasma in the magnetic field in solar corona, resulting in moving, reshaping, merging, or dispersing the magnetic fields in the solar atmosphere, leading to increased solar activity. Furthermore, when the planets are perfectly aligned, the tide is high and narrow; the rotating solar atmosphere would experience large tide force for a relatively short time. When the planets are only nearly aligned, the tide was not as high but broad; the solar atmosphere would continuously experience moderate tidal force for a relatively long time. The tidal effects would be significant in both cases.

The alignments of three or four planets from Mercury, Venus, Earth, and Jupiter were analyzed once a day from 1840 to 2019.

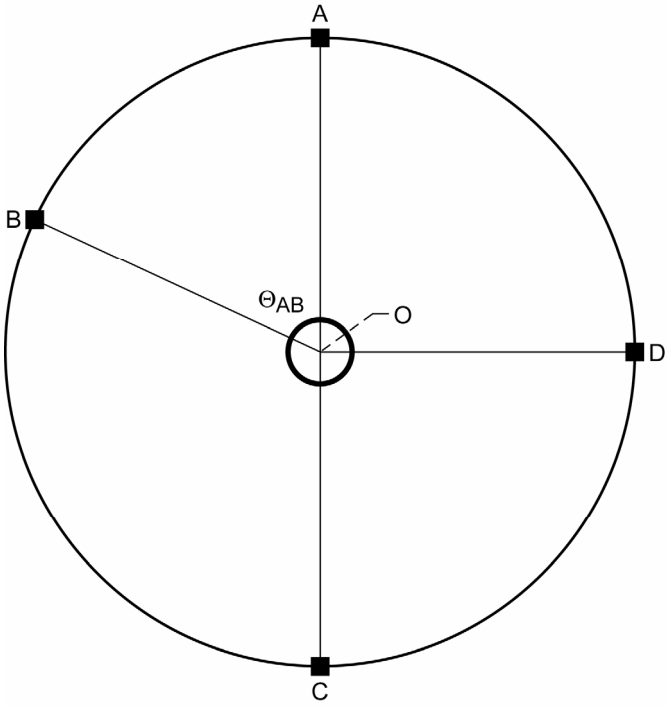

Figure 1.—Analysis of alignment of planets A, B, C, and D around Sun (centered at O).

Alignment Index: A Measure of Planet Alignment

In order to determine if there is a planet alignment, a measure to quantify the degree of planet alignment needs to be created. Such a system was devised as follows:

Figure 1 shows a situation of the Sun centered at point O and surrounded by four planets (A, B, C, and D), whose directions are as indicated. The alignment of planet A and the other three planets are examined individually. The alignment index I_{AX} for two planets A and X is defined as the cosine of the angle between A and X:

$$I_{AX} = \left|\cos \Theta_{AX}\right| \tag{2}$$

Therefore, the two planets have the highest index value of 1 when they are aligned ($\Theta_{AX} = 0$ or 180°), and lowest value of 0 when they are 90° apart.

The alignment index of planet A, I_A in a system of n planets, is defined as the sum of the alignment index for A and each individual planet:

$$I_A = \sum_{X=1}^{n} \left|\cos \Theta_{AX}\right| \tag{3}$$

Finally, the alignment I for the entire planet system is characterized by the index for the least aligned planet (I). That is,

$$I = \text{smallest among all } I_X$$

The planets are considered well aligned if the least-aligned planet is well aligned. That is, when the *I* value is high. In this situation all planets would produce one global tide that would be high or broad if the planets were well aligned or nearly aligned, respectively.

The above alignment index works best when these values are high. This research selected the high-value range of these indexes to identify and examine the days of high and broad global tides resulting from all planets.

Alignment Index Values From January 1, 1840, to May 31, 2019

The planet heliocentric ecliptic positions at 0:00 UT on every day from January 1, 1840, to May 31, 2019 (65 530 days), were obtained (ref. 15) and used to calculate the planet alignment indexes *I* described in the last section.

For the Mercury, Venus, Earth, and Jupiter four-planet system, the most-aligned 656 days (days of the top 1 percent *I* values) during this 180-year period were collected. Their distribution over this period is summarized in figure 2(a). The number of sunspots each year (ref. 21) is included in the figure. The figure does not reveal a clear cycle pattern. A fast Fourier transform (FFT) applied to the data (fig. 2(b)) indicated the data have a 7-year cycle. This cannot resonate with the 11-year solar activity cycle.

For the Venus, Earth, and Jupiter three-planet system, data show that these three planets become aligned with the Sun a few times in one continuous time period within a solar cycle and then become less aligned in another phase of the 11-year period (fig. 3(a)). The number of sunspots each year is again included. Its FFT indicates the cycle period was 11.07 years (fig. 3(b)) during this 180-year period. This compares with the 11.08 years claimed by Wood (ref. 5), 10.4 years claimed by Okal and Anderson (ref. 10), and average sunspot cycle of 10.92 years during the past 300 years (ref. 22).

The correlation between the sunspot cycle and the planet alignment cycle as illustrated in figure 3 was further examined by using more numerous alignment data. Instead of the top 1 percent most-aligned days, finding the cycle for the top 25 percent most-aligned days was conducted. The most-aligned day in this 25 percent was November 10, 1970. The heliocentric longitudes of Venus, Earth, and Jupiter were 47.3°, 47.6°, and 226.9°, respectively. The least-aligned day in this 25 percent was May 26, 1892, and the heliocentric longitudes of Venus, Earth, and Jupiter were, 218.3°, 246.7°, and 8.6°, respectively. Therefore, the “most-aligned days” here would include some days that the planets were aligned and some other days that they are only nearly aligned. This would give a more complete list of the days when the planet positions could possibly cause an increase of solar activity. Results after this modification show the sunspot cycle and the Venus-Earth-Jupiter alignment cycle are still quite similar (fig. 4). The FFT of the results described in figure 4, together with all other FFTs of the alignment data from the three-planet systems involving Mercury are summarized in figure 5. It appears that the tide caused by Mercury, by itself or in alignment with other planets, does not resonant with the 11-year solar cycle. This is to be expected because the number of days of planet alignment involving Mercury would not be large due to the fast movement of Mercury. Without resonance, the tide caused by Mercury cannot affect the 11-year solar cycle.

It is noted that figure 4 is very similar to the figure of planet alignment versus sunspot cycle presented by Wood (ref. 5). Wood’s results were criticized as incomplete and not convincing because it used only the most-aligned days (one in 0.8 years) for data analysis. Figure 4, however, was obtained using daily planet positions to select both the most-aligned days and the nearly aligned days as the days of significant tidal effects.

The small difference between the sunspot cycle period and the Venus-Earth-Jupiter alignment cycle period observed in this research could partly arise from the error due to the methodology used in this research. However, it is probable that the periods of these two cycles are, indeed, slightly different by amounts that are as irregular as the nontidal solar activities. This would lead to a complicated beat phenomenon. During the 1840 to 2005 study period when the 11-year sunspot cycle is obvious, the two cycles are in step as the planets are more aligned (i.e., more frequent high or broad global tides) at the

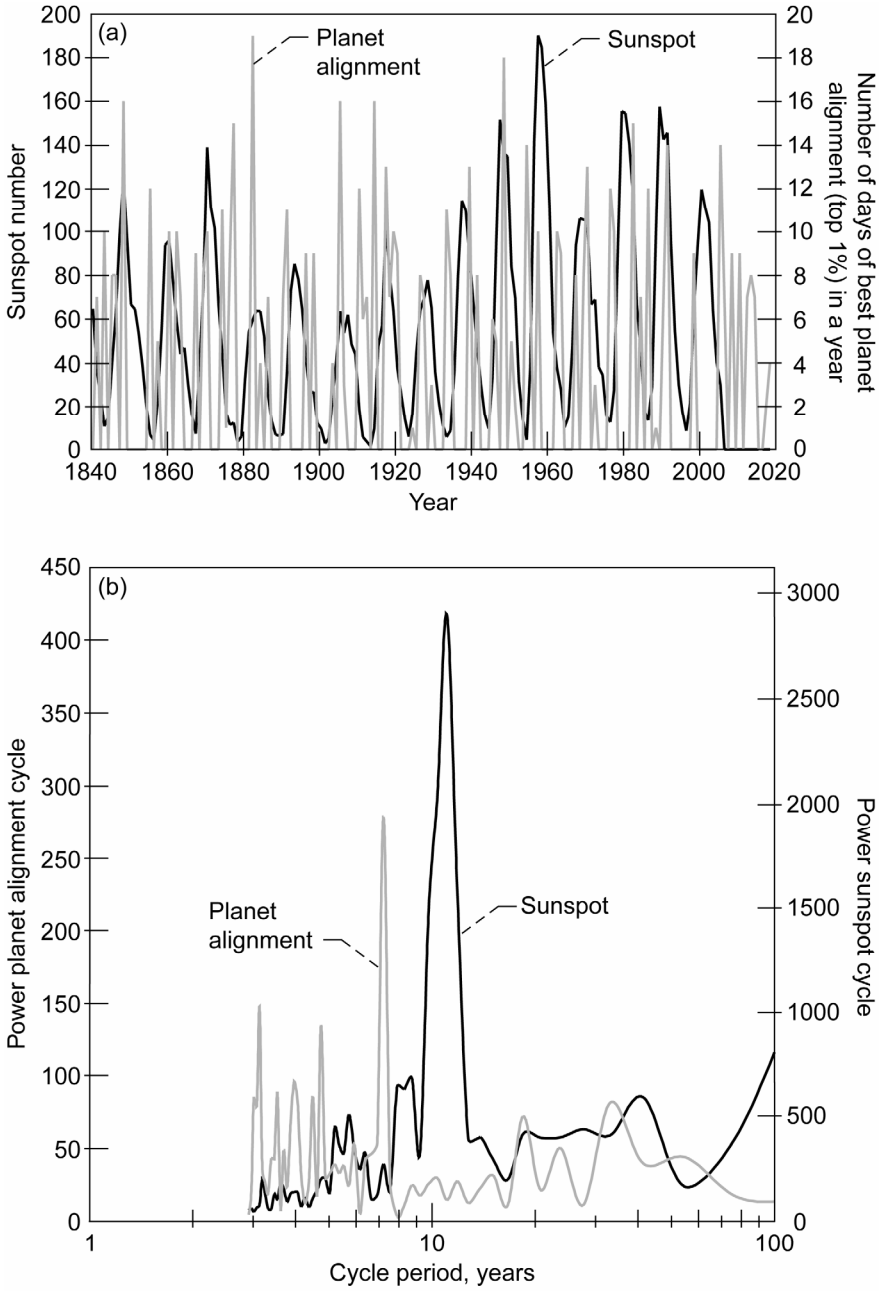

Figure 2.—Average number of sunspots every calendar year from 1840 to 2019 and number of most-aligned days (top 1 percent) each year for four-planet system Mercury, Venus, Earth, and Jupiter. (a) Number of sunspots and most-aligned days. (b) Fast Fourier transforms of number of sunspots and number of most-aligned days.

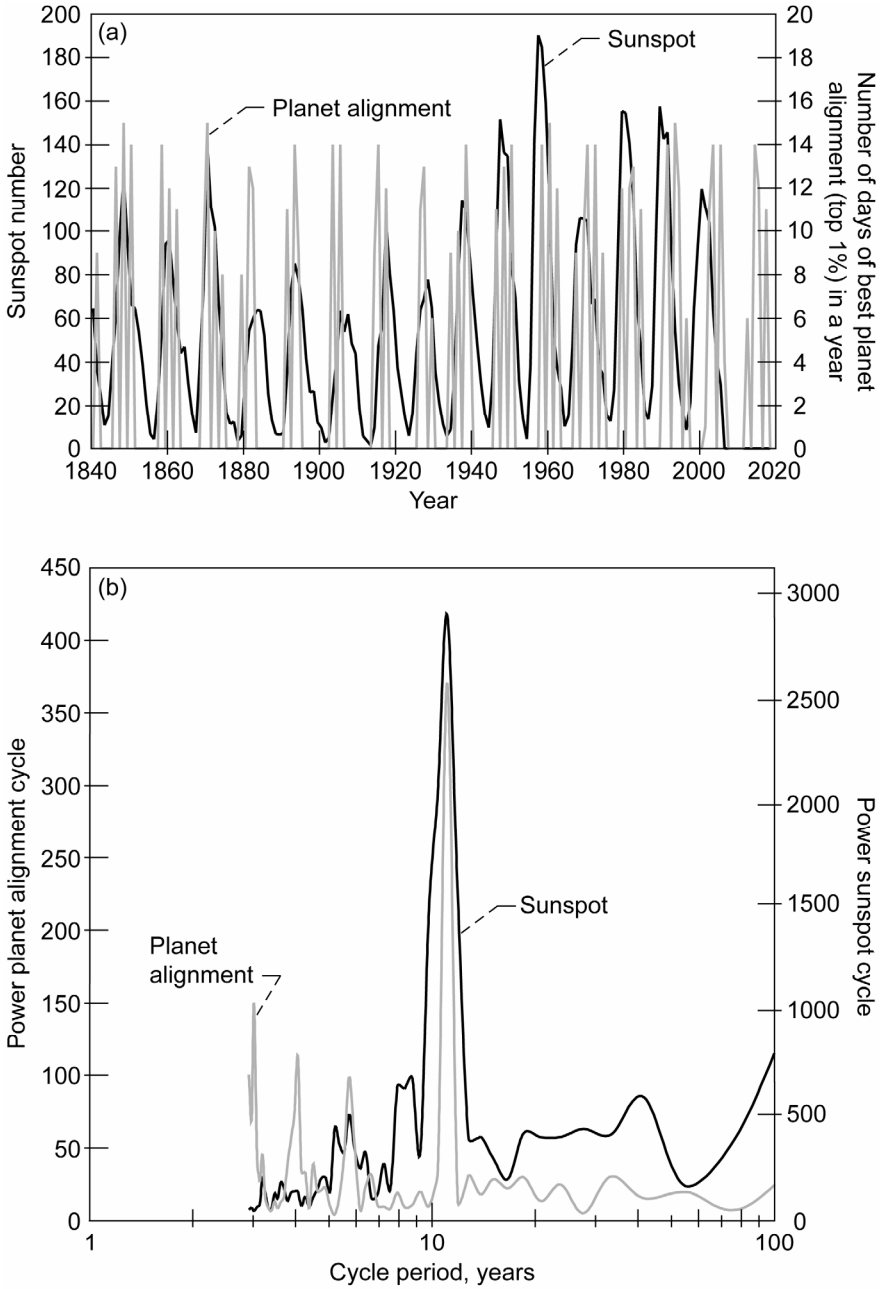

Figure 3.—Average number of sunspots every calendar year from 1840 to 2019 and number of most-aligned days (top 1 percent) each year for three-planet system Venus, Earth, and Jupiter. (a) Number of sunspots and most-aligned days. (b) Fast Fourier transforms of number of sunspots and number of most-aligned days.

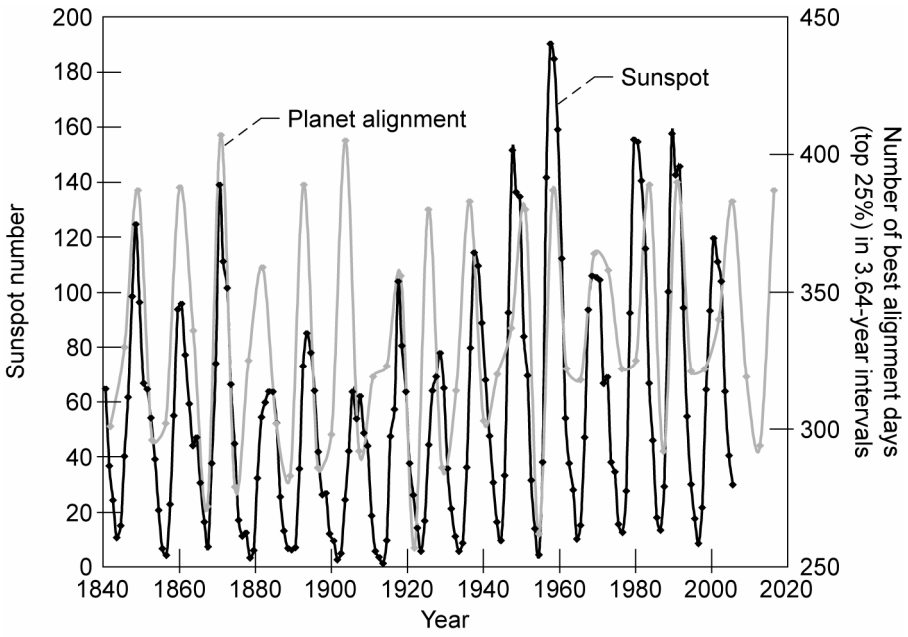

Figure 4.—Average number of sunspots every calendar year from 1840 to 2005 and number of most-aligned days (top 25 percent) each 3.64 years (1/3 of solar cycle) for Venus-Earth-Jupiter system from 1840 to 2018.

time near a solar maximum (fig. 4). The Maunder minimum, the period of 1645 to 1715 AD when few sunspots can be observed could be explained as the period when the solar activity cycle and the tidal cycle caused by the planet alignment were out of step for a long period of time.

It is further observed visually from figure 4 that the sunspot numbers are in general low during 1875 to 1930, when the planet alignment cycles are not in close step with the sunspot cycle. Alternatively, the sunspot numbers are the highest in the late 1950s, when the sunspot cycle and the planet alignment cycle are most closely in step. The observations are interesting and in agreement with the resonance-beat hypothesis. Looking into the future, it is nearing the solar minimum now (summer 2007), but the planet alignment will not reach minimum until 2012 (fig. 4). The apparent mismatch between these two minima would indicate these two cycles are out of step, and therefore a low sunspot number would be forecasted in the coming solar cycle 24, unless the current solar minimum would last for a few more years to reduce this mismatch.

Conclusions

In view of the statistics and the issues presented and discussed in this report, one must acknowledge the possibility that some type of tide-solar activity relation may truly exist, despite the widely accepted thought that believes otherwise.

Evidence of apparent relations between planet positions and solar activity was observed and presented:

(1) Twenty-five of the thirty-eight largest known solar flares were observed to start when one or more of the tide-producing planets (Mercury, Venus, Earth, and Jupiter) were either nearly above the event positions (<10° longitude) or at the opposing end of the Sun. The probability of this to happen at random is 0.039 percent. This observation supports the hypothesis that the force or momentum balance (between the solar atmospheric pressure, the gravitational field, and the magnetic field) on the plasma in the

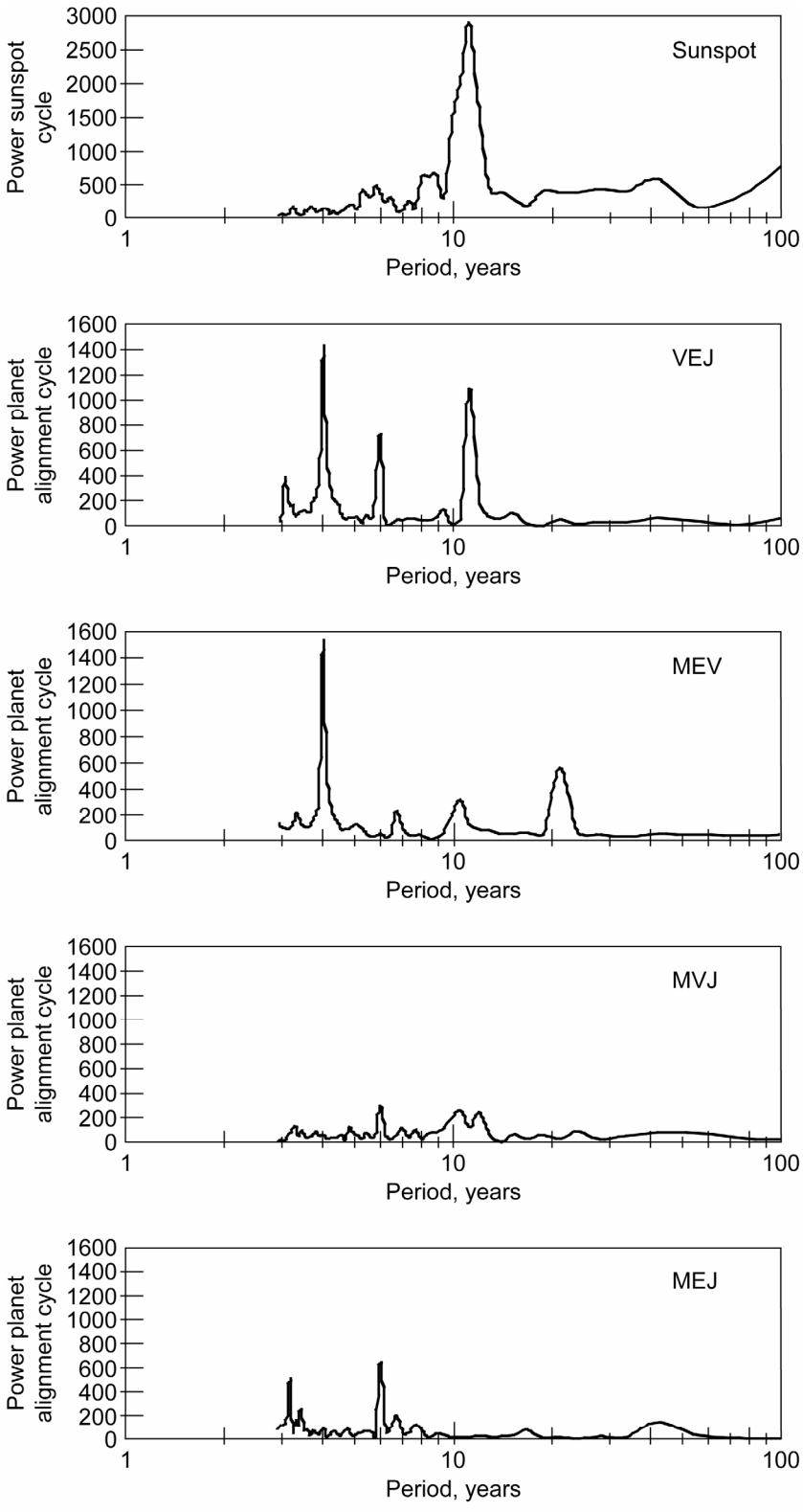

Figure 5.—Fast Fourier transforms of number of sunspots every calendar year from 1840 to 2005 and number of most-aligned days (top 25 percent) each 3.64 years (1/3 of solar cycle) for three-planet systems involving Mercury (M), Venus (V), Earth (E), and Jupiter (J).

looping magnetic field lines in solar corona could be disturbed by tides, resulting in magnetic field reconnection, solar flares, and solar storms.

(2) From the daily planet positions during the period from 1840 to 2000, an 11-year cycle of the alignment of Venus, Earth, and Jupiter is observed. This cycle approximately matches the sunspot cycle. When the two cycles were least matched, the sunspot numbers were low (1875 to 1930). When best matched, the sunspot numbers were high (late 1950s). This supports the hypothesis of resonance and beat between the cycle of small tides caused by the planet alignment and the cycle of independent, large, and irregular nontidal solar activity. Mercury produces significant tides, but is not considered because it does not have an 11-year-cycle resonance with the nontidal solar activities, either by itself or by aligning with other planets.

The observed relation between the predictable planet position and unpredictable solar flare suggests a way to forecast the times of the largest solar flares (X9.0 and larger, both near- and far-side from Earth) shortly after giant sunspots appear: They are most likely to start when these sunspots rotate into a region where at least one of the four tide-producing planets is either overhead or underfoot (within 10° longitude). They are least likely to occur when these sunspots are at 36° longitude or further away from the overhead or underfoot points of all these four planets.

The theory of resonance between the cycle of nontidal solar activity and the cycle of the alignment of Venus, Earth, and Jupiter forecast a low sunspot number in the coming solar cycle number 24 unless the current solar minimum would last for a few more years to reduce the current mismatch between these two cycles.

Further theoretical, instrumental, and statistical investigation is needed before there can be a final confirmation of the apparent relations observed in this research. One practical way to conduct a simple statistical study is to use the planet positions together with the available data and knowledge of solar physics to forecast, for the coming years, the solar flares in particular and solar activity in general. It would prove beneficial if such a prediction capability improves forecasting solar activity.

Appendix A
Tide Equations Relevant to This Report

According to the tide theory, the tide potential generated by a planet on a point at the Sun's surface (or any point in the solar atmosphere) (ref. 23) is approximately

$$U(r_s,\varphi)=\left(\frac{GM_p r_s^2}{R_{ps}^3}\right)\left(3\cos^2\varphi-1\right) \tag{A1}$$

where G is the gravitational constant, M_p is the mass of the planet, r_s is the radius of the Sun (or the distance from the Sun's center to the point in the solar atmosphere being examined), R_{ps} is the distance between the planet and the Sun's center, and φ is the angle westward from the direction of the planet to the point on the Sun's surface, as viewed from the center of the Sun.

From the above equation, the magnitude of the horizontal component (westward) of the tide-driving gravity by a planet on the point at the Sun's surface (ref. 23) is

$$g_h=\frac{1}{r_s}\left(\frac{\partial U}{\partial\varphi}\right) \tag{A2}$$

or from equation (A1),

$$g_h=-1\left(\frac{3}{2}\right)\left(\frac{GM_p r_s}{R_{ps}^3}\right)\sin 2\varphi \tag{A3}$$

It can be illustrated (ref. 24) that g_h points in a horizontal direction to a location directly under the planet on the Sun's surface or the opposing side, whichever is closer. This is shown in figure 6.

The magnitude of the upward vertical component of the tide-driving gravity by a planet on a point F (fig. 6) at the Sun's surface can also be calculated (ref. 23) as

$$g_v=\frac{\partial U}{\partial r_s} \tag{A4}$$

or from equation (A1),

$$g_v=\left(\frac{3}{2}\right)\left(\frac{GM_p r_s}{R_{ps}^3}\right)(\cos 2\varphi+1/3) \tag{A5}$$

The relative values of $GM_p r_s \big/ R_{ps}^3$ for Venus and Jupiter are about equal and are about twice of those for Mercury and Earth. The values of this term for all other planets are small and are not considered in this research. The last term in equation (A5) is a constant, 1/3. It represents the part of the vertical tide-driving gravity (g_v) that is independent of φ. This term may be neglected in tide analysis because it is much smaller than the Sun's own gravity, another vertical gravity that is independent of φ.

The tide-driving gravity calculated according to the above equations was compared with the affected body's own gravity. The ratios were 10^{-7} and 10^{-12} for the Earth's surface and Sun's photosphere, respectively.

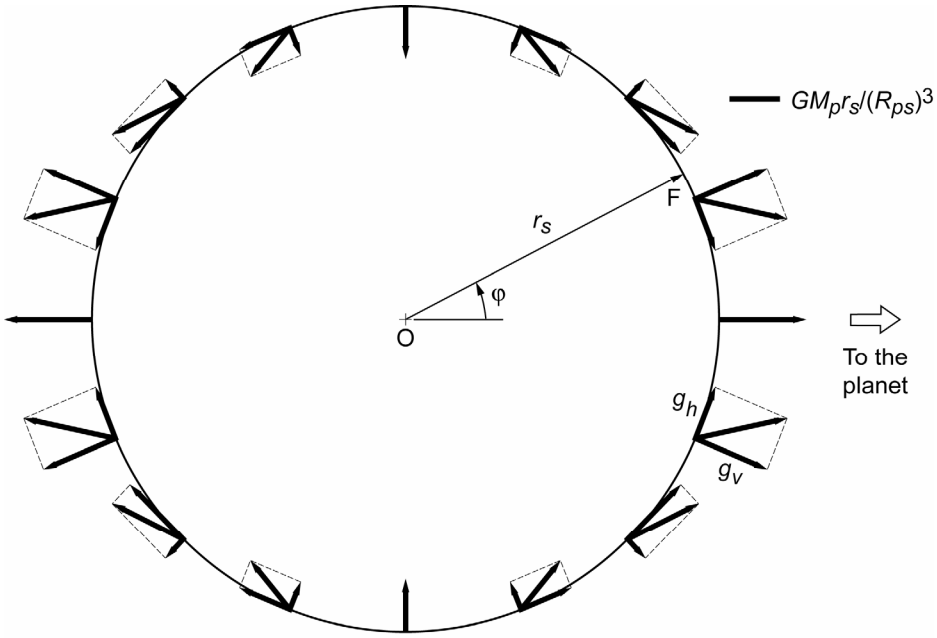

Figure 6.—Magnitude and direction of tide-driving gravities with their horizontal and vertical components (g_h and g_v, in equations (A3) and (A5), respectively) at different positions on surface of Sun. Scale at upper right represents magnitude of $GM_p r_s/(R_{ps})^3$ where G is gravitational constant, M_p is mass of tide-producing planet, r_s is radius of Sun, and R_{ps} is distance between planet and Sun's center. φ is angle westward from direction of planet to point F on Sun's surface. Tide-producing planet is off to right of figure.

Appendix B
Tidal Effects Caused by Rotation Period of Affected Body Relative to Tide-Producing Body

The atmosphere tide is characterized by pressure change. As a result of tide-driving gravity in the solar atmosphere, the pressure differences between the plasma in the magnetic fields and the materials outside would change because of their different environments (such as particle densities). Corresponding to a variation in state, the magnetic fields at some parts of the solar atmosphere could move, change shape, merge, or disperse; then the solar activity could increase or decrease. For example, in the looping magnetic field lines in solar corona, the balance between the atmospheric pressure and the magnetic field on masses of plasma could be disturbed by the pressure changes caused by tides. This could trigger magnetic field line reconnection or solar flare.

For the pressure inside and outside of the magnetic fields in the solar corona to change significantly, it may need to be under the influence of large tide-driving gravity (i.e., pressure increase due to high tide) for a length of time. If Newton's law of linear motion is used as a first-order approximation, then the distance an object (e.g., molecule or ion) could move (S) under the tide-driving gravity (g) over a time interval (T) is

$$S = 0.5gT^2 \tag{B1}$$

Therefore it is hypothesized that the changes of the solar activity caused by the tide-driving displacement of the hot plasma is proportional to the magnitude of the tide-driving gravity and to the square of the length of time when the active region is under the influence of the tide-driving gravity. This time interval is inversely proportional to the angular orbiting speed of the tide-producing body, or it is proportional to the rotation period of the affected body viewed from the tide-producing body. This time interval also depends on the alignment of the four tide-producing planets (Mercury, Venus, Earth, and Jupiter). For example, if these four planets are nearly aligned, together they will form a broad tide, and the length of time for the active region to be under the influence of the effective tide-driving gravity will be considerably longer than that caused by the tide of the individual planet.

The Sun's rotation period relative to those of the planets is about 25 to 35 times the Earth's rotation period. Compared with the tide on Earth, this parameter would favor large tidal effects on the Sun by a factor of about 625 to 1025. These effects would even be larger if the period of effective tides is prolonged because of near alignment of the planets.

Appendix C
Conversion of the Solar Flare Event Position From Heliographic Coordinates to Heliocentric Ecliptic Coordinates (for Data in Tables I to IV)

Examination of the solar flare position relative to planet position is an important part of this research. Since the solar flare position data and the planet position data are given in different coordinate systems (heliographic coordinates and heliocentric ecliptic coordinates, respectively), it is necessary to transform the solar flare positions from heliographic coordinates to heliocentric ecliptic coordinates.

By neglecting the angle between the Sun's equator and the ecliptic (7.25°), the heliocentric ecliptic longitude of a point on the Sun can quickly be obtained by adding heliographic longitude of the point (observed from Earth) to the heliocentric ecliptic longitude of the Earth. The errors caused by this approximation are usually less than 2°. This approximation is excellent for a quick analysis and was previously used by Schuster (ref. 7). For the purpose of illustrating that Schuster's method is a good approximation, the present report uses the following method that does not neglect the equator-ecliptic angle.

To do this, the solar flare position is at first transformed from heliographic coordinates to heliocentric Earth equatorial (HEEQ) coordinates as described by Thompson (ref. 20). It is then transformed from HEEQ to heliocentric Aries ecliptic (HAE) coordinates using the method given by Hapgood (ref. 19) and is finally transformed from HAE (equinox of the year) to heliocentric ecliptic (equinox of 2000 AD) coordinates. The complete process is as follows:

(1) From heliographic to HEEQ coordinates (ref. 20)

The heliographic coordinate is used for the event positions of the individual solar flares. In this coordinate system, the origin is at the intersection of the solar equator and the central meridian as seen from Earth. The latitude numbers (Θ) increase toward solar north. The longitude numbers (Φ) increase toward solar west.

The two-dimensional heliographic coordinates are used to identify a point on the Sun's surface. Therefore, its third dimension is r = the Sun's radius = r_s. These (polar) coordinates can then be converted to and from the (Cartesian) HEEQ coordinates according to the following equations:

$$r = \sqrt{X_{\mathrm{HEEQ}}^2 + Y_{\mathrm{HEEQ}}^2 + Z_{\mathrm{HEEQ}}^2} \tag{C1}$$

$$\Theta = \tan^{-1}\left(\frac{Z_{\mathrm{HEEQ}}}{\sqrt{X_{\mathrm{HEEQ}}^2 + Y_{\mathrm{HEEQ}}^2}}\right) \tag{C2}$$

$$\Phi = \tan^{-1}\left(\frac{X_{\mathrm{HEEQ}}}{Y_{\mathrm{HEEQ}}}\right) \qquad \text{if } X_{\mathrm{HEEQ}} > 0 \tag{C3a}$$

$$\Phi = \tan^{-1}\left(\frac{X_{\mathrm{HEEQ}}}{Y_{\mathrm{HEEQ}}}\right) + 180° \qquad \text{if } X_{\mathrm{HEEQ}} < 0 \text{ and } Y_{\mathrm{HEEQ}} > 0 \tag{C3b}$$

$$\Phi = \tan^{-1}\left(\frac{X_{\mathrm{HEEQ}}}{Y_{\mathrm{HEEQ}}}\right) - 180° \qquad \text{if } X_{\mathrm{HEEQ}} < 0 \text{ and } Y_{\mathrm{HEEQ}} > 0 \tag{C3c}$$

$$X_{\mathrm{HEEQ}} = r\cos\Theta\cos\Phi \tag{C4a}$$

$$Y_{\mathrm{HEEQ}} = r\cos\Theta\sin\Phi \tag{C4b}$$

$$Z_{\mathrm{HEEQ}} = r\sin\Theta \tag{C4c}$$

The (Cartesian) HEEQ coordinates have the origin at the Sun's center, the X-axis at the intersection between solar equator and solar central meridian as seen from Earth, and the Z-axis is the solar rotation axis pointing to the North Pole.

The "third dimension" $r = r_s$ can be used for the calculations in this research. However, this will be canceled out later when the Cartesian coordinate is transformed back to the two-dimensional polar coordinates (eq. (C14)). Therefore, $r = 1$ is used for the calculation in this report.

(2) From HEEQ to HAE (ref. 19)

In the (Cartesian) HAE coordinate system, the origin is the Sun's center. The Z-axis is perpendicular to the ecliptic (i.e., the Earth orbit), pointing toward north. The X-axis is in the ecliptic surface, pointing toward the First Point of Aries (i.e., the direction of the instantaneous equinox or the direction of the Sun viewed from Earth at the spring equinox).

Hapgood gave the method of coordinate transformation from HAE to HEEQ. In this research, the reverse transformation is needed. That is, the transformation from HEEQ to HAE.

The transform matrix developed by Hapgood is

$$\begin{bmatrix} \cos\theta & \sin\theta & 0 \\ -\sin\theta & \cos\theta & 0 \\ 0 & 0 & 1 \end{bmatrix}\begin{bmatrix} 1 & 0 & 0 \\ 0 & \cos\ell & \sin\ell \\ 0 & -\sin\ell & \cos\ell \end{bmatrix}\begin{bmatrix} \cos\Omega & \sin\Omega & 0 \\ -\sin\Omega & \cos\Omega & 0 \\ 0 & 0 & 1 \end{bmatrix}\begin{bmatrix} X_{\mathrm{HAE}} \\ Y_{\mathrm{HAE}} \\ Z_{\mathrm{HAE}} \end{bmatrix} = \begin{bmatrix} X_{\mathrm{HEEQ}} \\ Y_{\mathrm{HEEQ}} \\ Z_{\mathrm{HEEQ}} \end{bmatrix} \tag{C5}$$

Therefore, the inverse matrix is

$$\begin{bmatrix} \cos\Omega & \sin\Omega & 0 \\ -\sin\Omega & \cos\Omega & 0 \\ 0 & 0 & 1 \end{bmatrix}\begin{bmatrix} 1 & 0 & 0 \\ 0 & \cos\ell & \sin\ell \\ 0 & -\sin\ell & \cos\ell \end{bmatrix}\begin{bmatrix} \cos\theta & \sin\theta & 0 \\ -\sin\theta & \cos\theta & 0 \\ 0 & 0 & 1 \end{bmatrix}\begin{bmatrix} X_{\mathrm{HEEQ}} \\ Y_{\mathrm{HEEQ}} \\ Z_{\mathrm{HEEQ}} \end{bmatrix} = \begin{bmatrix} X_{\mathrm{HAE}} \\ Y_{\mathrm{HAE}} \\ Z_{\mathrm{HAE}} \end{bmatrix} \tag{C6}$$

where

θ is the angle of rotation in the plane of solar equator from the ascending node to the central meridian,

$$\theta(\mathrm{deg}) = \arctan(\cos\ell\,\tan(\lambda_{\odot} - \Omega))\ \text{(The quadrant of } \theta \text{ is opposite that of } \lambda_{\odot} - \Omega) \tag{C7}$$

ℓ is the angle of rotation from the plane of ecliptic to the solar equator,

$$\ell\ (\mathrm{deg}) = 7.25 \tag{C8}$$

Ω is the angle of rotation in the plane of ecliptic from the First Point of Aries to the ascending node of the solar equator,

$$\Omega(\mathrm{deg}) = 73.6667 + 0.013958\left(\frac{MJD + 3242}{365.25}\right) \tag{C9}$$

MJD, the modified Julian date, is the number of days measured from 00:00 UT on November 17, 1858 (Julian date 2400000.5), to 00:00 UT on the day of interest,

$\lambda_{\odot}$ is the Sun's ecliptic longitude,

$$\lambda_{\odot}(\text{deg}) = \Lambda + (1.915 - 0.0048T_0)\sin M + 0.020\sin 2M \tag{C10}$$

M is the Sun's mean anomaly,

$$M(\text{deg}) = 357.528 + 355999.050T_0 + 0.04107UT \tag{C11}$$

Λ is the Sun's mean longitude,

$$\Lambda(\text{deg}) = 280.460 + 36000.772T_0 + 0.04107UT \tag{C12}$$

UT is the number of hours in Universal Time on the day of interest, and

T_0 is the time in Julian centuries from 12:00 UT on 1 January 2000 to the previous midnight:

$$T_0 = \frac{MJD - 51544.5}{36525.0} \tag{C13}$$

(3) From HAE (Cartesian) to HAE (polar) coordinates

In the HAE (polar) coordinate, the origin is the Sun's center. The Earth orbit (ecliptic) is the plane of zero latitude. The direction of the X axis in the HAE Cartesian system is the direction of zero longitude. The latitude numbers (*Lat*) increase toward ecliptic north. The longitude numbers (*Lon*) increase toward ecliptic west. Therefore, the Cartesian to polar coordinate transformation is

$$Lat_{\text{HAE}} = \tan^{-1}\left(\frac{Z_{\text{HAE}}}{\sqrt{X_{\text{HAE}}^2 + Y_{\text{HAE}}^2}}\right) \tag{C14a}$$

$$Lon_{\text{HAE}} = \tan^{-1}\left(\frac{Y_{\text{HAE}}}{X_{\text{HAE}}}\right) \qquad \text{if } X_{\text{HAE}} > 0 \tag{C14b}$$

$$Lon_{\text{HAE}} = \tan^{-1}\left(\frac{Y_{\text{HAE}}}{X_{\text{HAE}}}\right) + 180° \qquad \text{if } X_{\text{HAE}} < 0 \tag{C14c}$$

(4) From HAE (polar) to heliocentric ecliptic equinox of J2000 (polar) ($\text{HAE}_{\text{J2000}}$) coordinates (ref. 19)

The only difference between these two coordinate systems is the definition of the point of zero longitude. The HAE (polar) has the zero longitude at the equinox at the date for which the data is calculated. This zero longitude position moves slowly, at a rate of about 1° longitude in 70 years. The $\text{HAE}_{\text{J2000}}$ coordinates have the zero longitude at the equinox at the date of January 1, 2000, AD. This zero longitude position does not move. The planet positions over the past 200 years are recorded using the $\text{HAE}_{\text{J2000}}$ coordinates. The latitude values of these two systems are the same.

$$Lat_{\mathrm{HAE_{J2000}}} = Lat_{\mathrm{HAE}} \tag{C15}$$

To transform a solar flare event longitude from HAE (polar) to heliocentric ecliptic equinox of J2000 (polar), an approximate equation can be derived based on equation (C9):

$$Lon_{\mathrm{HAE_{J2000}}} = Lon_{\mathrm{HAE}} + 0.013958(2000 - Y_{\mathrm{data}}) \tag{C16}$$

where Y_{data} is the calendar year (in AD) for the data point being examined.

Appendix D
Trial Forecast of Solar Flares

The appearance of the previous largest known solar flares followed a pattern, which is described in this report and again described briefly in the next paragraphs. It is hoped that this pattern can be used to forecast future large solar flares. A practical way to test this possibility is to use the observed pattern to make repeated trial forecasts in the coming months or years, and then compare the forecasts with the fact that are subsequently observed. This appendix describes the first of such trial forecasts and comparisons.

Based on data from past events, when giant sunspot groups appear it is seen that the largest solar flares (X9.0 and larger)

(A) are most likely to start when these sunspot groups rotate into a region where at least one of the four tide-producing planets (Mercury, Venus, Earth, or Jupiter) is either overhead or underfoot (within 10° longitude)

(B) are also likely to start when these sunspot groups are at 28° to 32° longitude away from the overhead or underfoot points of at least one of the four tide-producing planets

(C) are least likely to occur when these sunspot groups are at 36° longitude or further away from the overhead or underfoot points of all these four planets

These three rules were good in the past, but will they hold true in the future? The first opportunity to answer this question came when the very large sunspot group 960 rotated into the east limb of the solar disk on June 1, 2007, and the precondition for the above three rules was met (giant sunspot group appeared). In the following 2 weeks, actual solar flare events (C class and larger) associated with this sunspot group were recorded by satellites GOES10 and GOES11; the data are summarized in table V. Although the very large sunspot group decayed significantly after several days, the data in table V were nonetheless compared with solar flare forecasts made from the above three rules:

(a) Large solar flares were forecasted to start between late June 3 and early June 5, 2007, when the sunspot group 960 was rotated to overhead point of Mercury and Venus. They would also have been very likely to start on June 7 or 8, 2007, when the sunspot group was rotated to the position overhead of Earth and Jupiter.

As shown in table V, the largest solar flare (M8.9) for sunspot group 960 actually started at 5:06 a.m. UT on June 4, within the first forecasted time period, but there was no large solar flare in the next forecasted period (June 7 to 8). Instead, this second forecasted period was crowded with seven smaller (C-class) flares. It appears that the decaying sunspot group could not produce a large solar flare but was still strong enough to act with the tide to produce many smaller flares throughout this period.

(b) Based on the previous pattern, large solar flares would also have started when the sunspot group was 28° to 32° from any of the four tide-producing planets. These happened from late on June 1 to early on June 2, midday on June 5, midday and late on June 6, and midday on June 9.

Table V shows there were indeed solar flares in all of these time periods, when the sunspot group 960 was 28° to 32° from one or two of the four tide-producing planets. It is noted that the solar flare at 10:17 p.m. UT on June 1 happened as forecasted when the event position was 29° from Venus. However, it was 25° from Mercury, not the forecasted 28° to 32° range. Separately, the M1.0 solar flare on June 9 is most interesting because it happened at the time when the sunspot group had been significantly decayed for 5 days since the last M flare, and a new M-class flare looked less and less likely. Yet it was correctly forecasted based on the rules presented here when it started at 29° longitude from Jupiter at the start time of the flare.

(c) Large solar flares would have been least likely to occur both before June 1 and after midday on June 10, when the sunspot group was more than 36° longitude from all tide-producing planets.

TABLE V.—PLANET POSITIONS RELATIVE TO POSITION OF SOLAR FLARE EVENTS ASSOCIATED WITH SUNSPOT GROUP 960 IN JUNE 2007
[Recorded by satellites GOES10 and GOES11.]

Event position[a]		Flare intensity[b]	Date	Time, UT[c]	Ecliptic longitude[d]					Event position relative to high-tide positions[e]			
Latitude	Longitude				M	V	E	J	F	M	V	E	J
8S	89E	M1.0	1	6:46	195.9	201.0	250.3	254.4	161.4	–34	–40	–89	87
8S	89E	M2.8	1	14:35	197.0	201.5	250.6	254.5	161.7	–35	–40	–89	87
7S	89E	M2.1	1	21:40	198.1	202.0	250.9	254.5	162.0	–36	–40	–89	87
7S	78E	C2.8	1	22:17	198.1	202.0	250.9	254.5	172.9	–25	–29	–78	–82
8S	89E	M2.9	2	5:25	199.2	202.5	251.2	254.5	162.3	–37	–40	–89	88
4S	74E	M1.0	2	10:28	199.9	202.8	251.4	254.5	177.4	–22	–25	–74	–77
7S	66E	M2.4	3	1:51	202.1	203.9	252.0	254.6	185.9	–16	–18	–66	–69
8S	70E	M7.0	3	2:06	202.1	203.9	252.1	254.6	181.9	–20	–22	–70	–73
4S	64E	C1.6	3	2:31	202.2	203.9	252.1	254.6	188.0	–14	–16	–64	–67
5S	63E	M4.5	3	6:36	202.8	204.2	252.2	254.6	189.2	–14	–15	–63	–65
8S	67E	C5.3	3	9:23	203.2	204.4	252.3	254.6	185.2	–18	–19	–67	–69
5S	50E	M8.9	4	5:06	205.9	205.7	253.1	254.7	203.0	–3	–3	–50	–52
9S	37E	C1.2	5	4:15	209.1	207.2	254.1	254.7	216.4	7	9	–38	–38
9S	30E	C6.6	5	15:29	210.6	208.0	254.5	254.8	223.7	13	16	–31	–31
9S	14E	C9.7	6	16:55	213.9	209.7	255.5	254.9	240.5	27	31	–15	–14
8S	12E	C1.7	6	23:13	214.8	210.1	255.8	254.9	242.9	28	33	–13	–12
9S	8E	C3.9	7	6:22	215.7	210.6	256.1	254.9	247.0	31	36	–9	–8
9S	2E	C1.1	7	10:10	216.2	210.9	256.2	254.9	253.1	37	42	–3	–2
8S	2W	C1.6	8	1:31	218.1	211.9	256.8	255.0	257.7	40	46	1	3
8S	4W	C2.3	8	4:10	218.5	212.1	256.9	255.0	259.9	41	48	3	5
8S	3W	C1.4	8	4:55	218.6	212.1	257.0	255.0	258.9	40	47	2	4
8S	10W	C2.9	8	8:22	219.0	212.3	257.1	255.0	266.0	47	54	9	11
8S	9W	C1.5	8	14:09	219.8	212.7	257.3	255.0	265.2	45	52	8	10
9S	27W	M1.0	9	13:30	222.7	214.3	258.3	255.1	284.0	61	70	26	29
9S	40W	C1.9	10	11:01	225.4	215.7	259.1	255.2	298.0	73	82	39	43

[a]N, S, E, and W are north, south, east, and west, respectively.

[b]M-class flares are 10 times more intense than C-class. Higher numbers indicate higher intensity of x-ray emissions.

[c]UT is universal time.

[d]The Earth location at vernal equinox of 2000 AD is 180°. M, V, E, J, and F are Mercury, Venus, Earth, Jupiter, and flare, respectively.

[e]Position is in ecliptic longitude. Positive deviation means the event position was ahead (to the west) of the planet position. Negative deviation means the event position was behind (to the east) of the planet position. High-tide position is defined as the position where the associated planet is either overhead or underfoot.

Table V shows only one small (C1.9) flare having occurred during the time from June 10 to 14, when the sunspot group 960 was rotated from the west limb of the solar disk to the far side. It also shows several M-class solar flares having started on June 1 and 2, when the event position and the nearest planet (Mercury) was 34° to 37° apart. In this instance the actual solar flares happened outside of the forecasted zone, but only by a very small amount.

To summarize, it is noted that the forecast based on rules (A) and (B) worked very well, but the forecast based on rule (C) worked only marginally well. It is also noted that the solar flares from this sunspot group 960 (M8.9 and smaller) were much smaller than the flares from which rules (A), (B), and (C) were established (X9.0 and larger). In this particular forecast, applying these three rules to flares smaller than X9.0 produced acceptable results.

The trial forecast described here is a single data point that supports the possibility of forecasting the solar flares based on the planet positions, but it is far from statistically significant. Using the future large sunspot groups and the procedure described above to repeatedly conduct trial forecasts of solar flares is needed to confirm, disprove, or modify the above three rules of solar flare forecasting.

References

1. Odenwald, Sten F.: The 23rd Cycle: Learning to Live With a Stormy Star. Columbia University Press, New York, NY, 2001.
2. Holman, Gordon D.: The Mysterious Origins of Solar Flares. Sci. Amer., vol. 294, issue 4, 2006, p. 38.
3. Lang, Kenneth R.: The Cambridge Encyclopedia of the Sun. Cambridge University Press, Cambridge, UK, 2001.
4. Takahashi, K.: On the Relation Between the Solar Activity Cycle and the Solar Tital Force Induced by the Planets. Solar Phys., vol. 3, 1968, pp. 598–602.
5. Wood, K.D.: Sunspots and Planets. Nature, vol. 240, 1972, pp. 91–93.
6. Blizard, J.B.: Long Range Solar Flare Prediction. NASA CR–61316, 1969.
7. Schuster, Arthur: The Influence of Planets on the Formation of Sun-Spots. Proceedings of the Royal Society of London. Series A, Containing Papers of a Mathematical and Physical Character, vol. 85, no. 579, 1911, pp. 309–323.
8. Dingle, L.A.; Van Hoven, G.; and Sturrock, P.A.: Test for Planetary Influences on Solar-Activity. Solar Phys., vol. 31, no. 1, 1973, pp. 243–246.
9. Smythe, C.M.; and Eddy, J.A.: Planetary Tides During Maunder Sunspot. Nature, vol. 266, 1977, pp. 434–435.
10. Okal, E.; and Anderson, D.L.: Planetary Theory of Sunspots. Nature, vol. 253, 1975, pp. 511–513.
11. Shea, M.A.; and Smart, D.F.: A Summary of Major Solar Proton Events. Solar Phys., vol. 127, no. 2, 1990, pp. 297–320.
12. Carrington, Richard C.: Description of a Singular Appearance Seen in the Sun on September 1, 1859. Mon. Not. R. Astron. Soc., vol. 20, 1860, pp. 13–15.
13. NOAA National Geophysical Data Center (NGDC). http://www.ngdc.noaa.gov/stp/SOLAR/ftpsolarflares.html#halpha Accessed May 22, 2007.
14. NASA Space Weather Bureau: The Most Powerful Solar Flares Ever Recorded. http://www.spaceweather.com/solarflares/topflares.html Accessed May 22, 2007.
15. MICA: Multiyear Interactive Computer Almanac. Version 2.0, U.S. Naval Observatory, Aug. 2005.
16. NOAA National Geophysical Data Center (NGDC): Solar H-Alpha Flare Events, 1940s. http://www.ngdc.noaa.gov/stp/SOLAR/ftpsolarflares.html Accessed May 23, 2007.
17. Dodson, Helen W.; and Hedeman, E. Ruth: The Comprehensive Flare Index (cfi) 1955–1969, UAG–14. http://www.ngdc.noaa.gov/stp/SOLAR/uaglist.html Accessed May 23, 2007.
18. Dodson, Helen W.; and Hedeman, E. Ruth: Experimental Comprehensive Solar Flare Indices for Certain Flares, 1970–1974. UAG–52. http://www.ngdc.noaa.gov/stp/SOLAR/uaglist.html Accessed May 23, 2007.
19. Hapgood, M.A.: Space Physics Coordinate Transformations—A User Guide. Planet. Space Sci., vol. 40, no. 5, 1992, pp. 711–717.
20. Thompson, W.T.: Coordinate Systems for Solar Image Data. Astron. Astr., vol. 449, 2006, pp. 791–803.
21. SIDC—Solar Influences Data Analysis Center: Monthly Report on the International Sunspot Number. Royal Observatory of Belgium World Data Center for the Sunspot Index, 2003. http://www.sidc.be/sunspot-data/ Accessed May 23, 2007.
22. Hathaway, D.H.; and Wilson, R.M.: What the Sunspot Record Tells Us About Space Climate. Solar Phys., vol. 224, no. 1, 2004, pp. 5–19.
23. Cartright, David Edgar: Tides: A Scientific History. Cambridge University Press, Cambridge, UK, 1999.
24. Tsantes, E.: Note on Tides. Amer. J. Phys., vol. 42, no. 4, 1974, pp. 330–333.

REPORT DOCUMENTATION PAGE	Form Approved OMB No. 0704-0188

1. REPORT DATE *(DD-MM-YYYY)*	2. REPORT TYPE	3. DATES COVERED *(From - To)*
13-07-2007	Technical Memorandum	

4. TITLE AND SUBTITLE
Apparent Relations Between Solar Activity and Solar Tides Caused by the Planets

5a. CONTRACT NUMBER

5b. GRANT NUMBER

5c. PROGRAM ELEMENT NUMBER

6. AUTHOR(S)
Hung, Ching-Cheh

5d. PROJECT NUMBER

5e. TASK NUMBER

5f. WORK UNIT NUMBER
WBS 698671.02.03.03

7. PERFORMING ORGANIZATION NAME(S) AND ADDRESS(ES)
National Aeronautics and Space Administration
John H. Glenn Research Center at Lewis Field
Cleveland, Ohio 44135-3191

8. PERFORMING ORGANIZATION REPORT NUMBER
E-15714-2

9. SPONSORING/MONITORING AGENCY NAME(S) AND ADDRESS(ES)
National Aeronautics and Space Administration
Washington, DC 20546-0001

10. SPONSORING/MONITORS ACRONYM(S)
NASA

11. SPONSORING/MONITORING REPORT NUMBER
NASA/TM-2007-214817

12. DISTRIBUTION/AVAILABILITY STATEMENT
Unclassified-Unlimited
Subject Category: 92
Available electronically at http://gltrs.grc.nasa.gov
This publication is available from the NASA Center for AeroSpace Information, 301-621-0390

13. SUPPLEMENTARY NOTES

14. ABSTRACT

A solar storm is a storm of ions and electrons from the Sun. Large solar storms are usually preceded by solar flares, phenomena that can be characterized quantitatively from Earth. Twenty-five of the thirty-eight largest known solar flares were observed to start when one or more tide-producing planets (Mercury, Venus, Earth, and Jupiter) were either nearly above the event positions (<10° longitude) or at the opposing side of the Sun. The probability for this to happen at random is 0.039 percent. This supports the hypothesis that the force or momentum balance (between the solar atmospheric pressure, the gravity field, and magnetic field) on plasma in the looping magnetic field lines in solar corona could be disturbed by tides, resulting in magnetic field reconnection, solar flares, and solar storms. Separately, from the daily position data of Venus, Earth, and Jupiter, an 11-year planet alignment cycle is observed to approximately match the sunspot cycle. This observation supports the hypothesis that the resonance and beat between the solar tide cycle and nontidal solar activity cycle influences the sunspot cycle and its varying magnitudes. The above relations between the unpredictable solar flares and the predictable solar tidal effects could be used and further developed to forecast the dangerous space weather and therefore reduce its destructive power against the humans in space and satellites controlling mobile phones and global positioning satellite (GPS) systems.

15. SUBJECT TERMS
Solar activity; Solar flare; Sunspot cycle

16. SECURITY CLASSIFICATION OF:			17. LIMITATION OF ABSTRACT	18. NUMBER OF PAGES	19a. NAME OF RESPONSIBLE PERSON
a. REPORT	b. ABSTRACT	c. THIS PAGE			Ching-Cheh Hung
U	U	U		32	19b. TELEPHONE NUMBER *(include area code)* 216-433-2302